Molecular Pharmacology Fast Forward. Published on February 21, 2013 as doi:10.1124/mol.112.083535

Title page

Molecular mechanism regulating 24-hour rhythm of dopamine D3 receptor expression in mouse ventral striatum

Eriko Ikeda, Naoya Matsunaga, Keisuke Kakimoto, Kengo Hamamura, Akane Hayashi, Satoru Koyanagi and Shigehiro Ohdo

Department of Pharmaceutics, Graduate School of Pharmaceutical Sciences, Kyushu University, Fukuoka, Japan (E.I., N.M., K.K., K.H., A.H., S.K., S.O.)

Molecular Pharmacology Fast Forward. Published on February 21, 2013 as DOI: 10.1124/mol.112.083535
This article has not been copyedited and formatted. The final version may differ from this version.

Running title page

Running title; REV-ERBα regulation of the 24-h rhythm of DRD3

Corresponding author: Shigehiro Ohdo, Ph.D. Department of Pharmaceutics, Graduate School of Pharmaceutical Sciences, Kyushu University, Fukuoka, 812-8582, Japan
Phone: +81-92-642-6612; FAX: +81-92-642-6613; E-mail: ohdo@phar.kyushu-u.ac.jp

The number of text pages; 35

The number of tables; 0

The number of figures; 6

The number of references; 37

The number of words in the *Abstract*; 249

The number of words in the *Introduction*; 547

The number of words in the *Discussion*; 1044

Abbreviations;DRD3; dopamine D3 receptor, RORα; retinoic acid-related orphan receptor, RORE; ROR response element, Per; period, Cry; Cryptochrome, Dbp; D-site binding protein, 7-OH-DPAT; 7-hydroxy-*N*,*N*-dipropyl-2-aminotetralin,

Molecular Pharmacology Fast Forward. Published on February 21, 2013 as DOI: 10.1124/mol.112.083535
This article has not been copyedited and formatted. The final version may differ from this version.

Abstract

The dopamine D3 receptor (DRD3) in the ventral striatum is thought to influence motivation and motor functions. Although the expression of DRD3 in the ventral striatum has been shown to exhibit 24-h variations, the mechanisms underlying the variation remain obscure. Here, we demonstrated that molecular components of the circadian clock act as regulators that control the 24-h variation in the expression of DRD3. The transcription of *DRD3* was enhanced by the retinoic acid-related orphan receptor α (RORα), and its activation was inhibited by the orphan receptor REV-ERBα, an endogenous antagonist of RORα. The serum or dexamethasone-induced oscillation in the expression of *DRD3* in cells was abrogated by the downregulation or overexpression of REV-ERBα, suggesting that REV-ERBα functions as a regulator of *DRD3* oscillations in the cellular autonomous clock. Chromatin immunoprecipitation assays of the *DRD3* promoter indicated that the binding of the REV-ERBα protein to the *DRD3* promoter increased in the early dark phase. DRD3 protein expression varied with higher levels during the dark phase. Moreover, the effects of the DRD3 agonist 7-hydroxy-*N*,*N*-dipropyl-2-aminotetralin (7-OH-DPAT)-induced locomotor hypoactivity were significantly increased when DRD3 proteins were abundant. These results suggested that RORα and REV-ERBα consist of a reciprocating mechanism wherein RORα upregulates the expression of DRD3, whereas REV-ERBα periodically suppresses the expression at the time of day when

Molecular Pharmacology Fast Forward. Published on February 21, 2013 as DOI: 10.1124/mol.112.083535
This article has not been copyedited and formatted. The final version may differ from this version.

REV-ERBα is abundant. Our present findings revealed that a molecular link between the circadian clock and the function of DRD3 in the ventral striatum acts as a modulator of the pharmacological actions of DRD3 agonists/antagonists.

Molecular Pharmacology Fast Forward. Published on February 21, 2013 as DOI: 10.1124/mol.112.083535
This article has not been copyedited and formatted. The final version may differ from this version.

Introduction

Most living organisms exhibit various biological rhythms that have a period length of approximately 24 h. Some of these rhythms are controlled by a self-sustained oscillation mechanism called the circadian clock. The master clock in the suprachiasmatic nuclei of the anterior hypothalamus in mammals is entrained to a 24-h period by the daily light/dark cycle. The master clock, in turn, synchronizes circadian oscillators in other brain regions and many peripheral tissues through neural and/or hormonal signals (Ohdo et al., 2011; Paul et al., 2011). Synchronized oscillators in peripheral tissues drive energy metabolism, cell division, hormonal secretion, and immune response (Matsuo et al,. 2003; Ishida et al., 2005; Shimba et al., 2005; Hashiramoto et al., 2010). The core circadian oscillator is composed of interacting positive and negative transcription/translational feedback loops. The *CLOCK* gene encodes the transcription factor, CLOCK, which dimerizes with BMAL1 to activate the transcription of Period (*Per1, Per2*) and Cryptochrome (*Cry1, Cry2*) genes through an E-box enhancer element (Gekakis et al., 1998; Kume et al., 1999). Once PER and CRY proteins have reached a critical concentration, they attenuate *CLOCK/BMAL1* transactivation, thereby generating a 24-h oscillation of their own transcription. An additional feedback loop that is believed to improve the robustness of the above description involves the orphan nuclear receptor REV-ERBα and the retinoic acid-related orphan receptor (ROR)-α. The interlocked loop, which consists of REV-ERBα and ROR, modulates the

Molecular Pharmacology Fast Forward. Published on February 21, 2013 as DOI: 10.1124/mol.112.083535
This article has not been copyedited and formatted. The final version may differ from this version.

transcriptional activity of the *Bmal1* gene (Preitner et al., 2002). These machineries regulate the 24-h variation in output physiology through the periodic expression of clock-controlled genes (Jin et al., 1999; Oishi et al., 2003).

Dopamine neurons are implicated in the regulation of voluntary movement and motivated behaviors through dopamine receptors (DRs) (Missale et al., 1998). DRs are grouped into 2 major classes, the D_1-like receptors (DRD1and DRD5) and the D_2-like receptors (DRD2, DRD3 and DRD4). The former is coupled to Gαs-proteins, whereas the latter is generally coupled to Gαi-proteins (Civelli et al., 1993; Gingrich et al., 1993). The dopamine D3 receptor (DRD3) is highly expressed in the ventral striatum, including the nucleus accumbens and the islands of Calleja (Bouthenet et al., 1991; Diaz et al., 2000). In knockout studies and experiments that have specifically investigated the role of DRD3, it has been postulated that DRD3 may mediate emotional behavior in mice (Xu et al., 1997). In addition, DRD3 in the ventral striatum has an important role in the treatment of many neurological diseases including depression, schizophrenia and Parkinson's disease (Gurevich et al., 1997; Joyce et al.,2001; Bézard et al., 2003). Thus, agonists/antagonists with reasonable selectivity for the D3 receptor subtype may improve the symptoms of these diseases. Recently, it has been reported that the levels of expression of DRD3 protein in the mouse striatum exhibit 24-h variations, and this rhythmicity could account for dosing time-dependent changes in the DRD3 agonist quinpirole, which induces

Molecular Pharmacology Fast Forward. Published on February 21, 2013 as DOI: 10.1124/mol.112.083535
This article has not been copyedited and formatted. The final version may differ from this version.

locomotor behaviors in mice (Akhisaroglu et al., 2005). However, the mechanisms underlying the 24-h variation in the levels of DRD3 expression remain unknown.

We describe here a circadian clock-controlled output pathway that promotes the expression of the *DRD3* gene. The RORα and REV-ERBα proteins inversely regulate the expression of the *DRD3* gene. This is the first description of the mechanism by which transcription of the *DRD3* gene is regulated by molecular components of the circadian clock.

Molecular Pharmacology Fast Forward. Published on February 21, 2013 as DOI: 10.1124/mol.112.083535
This article has not been copyedited and formatted. The final version may differ from this version.

Materials and Methods

Cells and Animals. Primary neurons or astrocytes were isolated from the mouse brain according to a previously published protocol (Reuss et al., 1998). In brief, mouse whole brain tissues from ICR E14.5 embryos were processed according to the above protocol for neurons and seeded at 1.3×10^4 cells/cm^2 in plastic flasks. After culturing for 24 h at 37 °C in a humidified 5% CO_2 atmosphere in Dulbecco's modified Eagle's medium (DMEM) that was supplemented with 10% fetal bovine serum (FBS), nonadherent cells were washed off, and adherent cells were further cultured in the same medium, which was changed every 3–4 days. After 10–14 days in culture, the floating nonastrocytic cells were removed from the underlying astrocyte monolayer by gentle shaking. The adherent cells were subcultured more than 2 times by trypsinization and seeded at a density of 3×10^4 cells/cm^2 in the same medium. After about 2 weeks, the astrocyte monolayer reached confluence. A mouse C-1300 neuroblastoma (C-1300N) cell line was purchased from RIKEN BioResource Center Cell Bank (Tsukuba, Japan). C-1300N cells were maintained in DMEM that was supplemented with 10% FBS at 37 °C in a humidified 5% CO_2 atmosphere. C-1300N cells were grown to confluence and synchronized with 100 nM dexamethasone (DEX) (Wako Pure Chemical Industries, Ltd., Osaka, Japan). NIH3T3 cells were supplied by the Cell Resource Center for Biomedical Research, Tohoku University (Sendai, Japan). NIH3T3 cells were transfected with pcDNA3.1 intact vector or pcDNA3.1 human drd3

Molecular Pharmacology Fast Forward. Published on February 21, 2013 as DOI: 10.1124/mol.112.083535
This article has not been copyedited and formatted. The final version may differ from this version.

using electroporation (Supplemental Method). ICR mice (5 weeks old) were purchased from Charles River Japan, Inc. (Kanagawa, Japan). Mice were housed under a 12-h light/dark cycle [lights on 7:00 at Zeitgerber time (ZT) 0] at a room temperature of 24 ± 1 °C and humidity of 60 ± 10% with food and water available ad libitum. All mice were adapted to the light/dark cycle for 2 weeks before the experiments and killed at 7 weeks old. During the dark period, a dim red light was used to aid treatment (<8 lux). In order to explore the influence of dosing time on the ability of the 7-hydroxy-*N*,*N*-dipropyl-2-aminotetralin (7-OH-DPAT) to inhibit the locomotor activity count, 7-OH-DPAT (Sigma-Aldrich Co. LLC, St. Louis, MO) was dissolved in saline at a concentration of 1 mg/mL and administered intraperitoneally in doses of 10, 50, or 100 μg/kg body weight at ZT2 or 14. Saline served as the control injection. All animal experiments and handling proceeded with the permission of the Animal Care and Use Committees of Kyushu University (Fukuoka, Japan).

Construction of reporter plasmids and expression plasmids. For the transcriptional assay, a fragment of the mouse *DRD3* gene spanning -2427 to +110 (the number is the distance in base pairs from the putative transcription start site, +1; GenBank accession No. NM_007877) was fused to the luciferase gene in the pGL4.12-Basic vector [DRD3 (-2427)-Luc] (Life Technologies Corporation, Grand Island, NY). The expression plasmids of CLOCK, BMAL1, PER2, REV-ERBα, and RORα were obtained by reverse transcription-polymerase chain reaction (RT-PCR) and used after their sequences were confirmed. All coding regions were ligated into the pcDNA3.1

Molecular Pharmacology Fast Forward. Published on February 21, 2013 as DOI: 10.1124/mol.112.083535
This article has not been copyedited and formatted. The final version may differ from this version.

vector (Life Technologies Corporation).

Transcription Assays. In order to explore whether the molecular components of the circadian clock regulate the expression of *DRD3*, the influence of clock gene products on the transcriptional activity of the *DRD3* gene was assessed by the overexpression of clock genes in C-1300N cells or by the luciferase reporter assay on constructs containing various lengths of the 5′-flanking region of the *DRD3* gene. C-1300N cells were transfected with 100 ng of reporter constructs and 2.0 μg (total) of expression vector with Lipofectamine LTX (Life Technologies Corporation). In order to correct for variations in transfection efficiency, 0.5 ng of pRL-TK vector (Promega Corporation, Madison, WI) was cotransfected in all Luciferase experiments. The total amount of DNA per well was adjusted with the pcDNA3.1 vector. Cell extracts were prepared 24 h after transfection with 200 μL of passive lysis buffer (Promega Corporation), and firefly luciferase and *Renilla reniformis* luciferase were assayed by luminometry in 20 μL of the extracts. The ratio of firefly (expressed from a reporter construct) to *R. reniformis* (expressed from pRL-TK) luciferase activities in each sample served as a measure of normalized luciferase activity.

small interfering RNA (siRNA). The siRNA of the mouse *REV-ERBα* gene were designed by Life Technologies Corporation. The siRNA oligonucleotide sequences were as follows: REV-ERBα siRNA sense, 5′-UUCCAUGGCCACUUGUAGACUUCCU-3′ and antisense,

Molecular Pharmacology Fast Forward. Published on February 21, 2013 as DOI: 10.1124/mol.112.083535
This article has not been copyedited and formatted. The final version may differ from this version.

5′-AGGAAGUCUACAAGUGGCCAUGGAA-3′; control siRNA sense, 5′-UUCCCAGGAAUACUCGAUUCCAACG-3′ and antisense, 5′-CGUUGGAAUCGAGUAUUCCUGGGAA-3′. The oligonucleotides were transfected into astrocyte cells at a final concentration of 100 pmol/mL with Lipofectamine 2000 (Life Technologies Corporation) according to the manufacturer's protocols.

Real-Time Monitoring of Circadian Bioluminescence. We tracked bioluminescence in C-1300N cells that were transfected with *DRD3*::*Luc* reporter vectors. Thereafter, cells were stimulated with 100 nM DEX for 2 h in order to synchronize their circadian clocks. Bioluminescence from *DRD3*::*Luc*-transfected cells or *Bmal1*::*Luc*-transfected cells was recorded with a real-time monitoring system (Lumicycle, Actimetrics, Wilmette, IL), and its amplitude was calculated with Lumicycle analysis software (Actimetrics). In order to explore the role of REV-ERBα in the rhythmic expression of *DRD3*, C-1300N cells were transfected with REV-ERBα. Thereafter, bioluminescence in the cells was recorded as described above.

Dissection of Brain Structures. Using stereotaxic coordinates (Franklin et al., 1997), a block of approximately 1 mm^3 (L1.0–L2.0, A0.7–A1.7 with 1-mm height) was taken out as the ventral striatum.

Real-time RT-PCR analysis. Total RNA was extracted from cultured cells and the mouse ventral striatum with RNAiso (Takara Bio Inc., Otsu, Japan). A real-time quantitative RT-PCR

Molecular Pharmacology Fast Forward. Published on February 21, 2013 as DOI: 10.1124/mol.112.083535
This article has not been copyedited and formatted. The final version may differ from this version.

assay was performed with the One Step SYBR PrimeScript RT-PCR Kit II (Takara Bio Inc.) and the 7500 Real-time PCR system (Life Technologies Corporation). Results were analyzed with 7500 system software (Life Technologies Corporation) with a standard curve. The relative *DRD3* RNA levels were normalized to the corresponding *β-actin* RNA levels. Relative RNA levels were expressed as a percentage of the maximal value that was obtained in each experiment. The sequence primer pairs were as follows: mouse *DRD3*, 5′-CCTCTGAGCCAGATAAGCAGA-3′ and 5′-AGACCGTTGCCAAAGATGATG-3′; mouse *β-actin*, 5′-GACGGCCAGGTCATCACTATT-3′ and 5′-TACCACCAGACAGCACTGTGT-3′. In order to investigate the temporal profiles of the intentional expression of *DRD3* mRNA, cell lysates from the ventral striatum of mice were prepared at ZT2, 6, 10, 14, 18, and 22.

Determination of locomotor activity. Locomotor activity data were measured with a photobeam activity system (ACTIMO-100; SHINTECHNO, Fukuoka, Japan), and activity counts were recorded at 1-min intervals. Activity counts were calculated with a moving average with a 30-min window except for the first 5 min; 7-OH-DPAT (10, 50, or 100 μg/kg, i.p.) was dissolved in saline.

Western blot analysis. In order to investigate the temporal profiles of the intentional expression of DRD3, RORα and REV-ERBα in the mouse ventral striatum, nuclear fractions of the ventral striatum were prepared at ZT2, 6, 10, 14, 18, and 22. Cell membranes or nuclear fractions

Molecular Pharmacology Fast Forward. Published on February 21, 2013 as DOI: 10.1124/mol.112.083535
This article has not been copyedited and formatted. The final version may differ from this version.

containing 20 µg of total protein were resolved by 10% (DRD3) or 8% (RORα and REV-ERBα) sodium dodecyl sulfate-polyacrylamide gel electrophoresis and transferred to a polyvinylidene difluoride membrane that was reacted with antibodies against DRD3, RORα (sc-9114 and sc-28612, both from Santa Cruz Biotechnology, Inc., Santa Cruz, CA), REV-ERBα (#2124, Cell Signaling Technology Japan, K.K., Tokyo, Japan), ACTIN, or RNA POLYMERASE 2 (sc-1616 and sc-899,both from Santa Cruz Biotechnology, Inc.). The molecular weights of DRD3, RORα , and REV-ERVα are 44 kDa, 67 kDa, and 80 kDa, respectively. These antibodies have been used in other published studies (Everett et al., 2010; Bugge et al., 2012; Ozaki et al., 2012). Specific antigen-antibody complexes were visualized with horseradish peroxidase-conjugated secondary antibodies and Chemi-Lumi One (Nakarai Tesque, Inc., Kyoto, Japan).

Chromatin Immunoprecipitation assay. In order to analyze the temporal binding of endogenous RORα and REV-ERBα on the *DRD3* promoter in the mouse ventral striatum, a chromatin immunoprecipitation (ChIP) assay was performed at ZT2, 10, 14 and 22. Ventral striatum segments were excised and treated with 8% formaldehyde for 5 min at room temperature in order to crosslink the chromatin. Each cross-linked sample was sonicated on ice and then incubated with antibodies against RORα (sc-28612, Santa Cruz Biotechnology, Inc.) and REV-ERBα (#2124, Cell Signaling Technology, Japan, K.K.). Chromatin/antibody complexes were extracted with a protein G agarose kit (Roche, Basel, Switzerland). DNA was

isolated with the Wizard SV Genomic DNA Purification System (Promega Corporation) and subjected to PCR using the following primer for the D-site of the *DRD3* promoter region: 5′-CTCTCATACCATCGCATGT-3′ and 5′-GCACAAAAGGTCTCACTCCT-3′. DNA was amplified with a Go Taq Green Master Mix (Promega Corporation). The PCR products were run on a 2% agarose gel. The gel was photographed with a digital camera after staining with ethidium bromide. For negative controls, chromatin immunoprecipitation was performed in the absence of antibody or in the presence of rabbit IgG. PCR products from these samples were not detectable by ethidium bromide staining. The relative ChIP PCR abundance was normalized to the corresponding input DNA levels.

Statistical analysis. The significance of the 24-h variations in each parameter was tested by a cosinor analysis with ChronoLab software. The rhythm characteristics that are estimated by this method include the acrophase (time of peak value in the fitted cosine function that is expressed as the lag in hours and minutes from midnight). *P* values that were determined from comparisons of the residuals before and after cosine curve fitting and that were less than 0.05 indicated the detection of a rhythm. The statistical significance of the differences among the groups was analyzed with ANOVA and Tukey's multiple comparison test. Probabilities that were less than 5% were considered significant.

Molecular Pharmacology Fast Forward. Published on February 21, 2013 as DOI: 10.1124/mol.112.083535
This article has not been copyedited and formatted. The final version may differ from this version.

Results

Transcriptional regulation of *DRD3* by clock gene products. In order to explore whether the products of clock genes and/or clock-controlled output genes affect the expression of *DRD3*, we performed a transient transcriptional assay with a *DRD3* luciferase reporter. Several putative binding motifs were located from 2427 bp upstream to 110 bp downstream from the transcription start site of the mouse *DRD3* gene (Fig. 1A). In order to investigate the functional importance of these sequences for the expression of *DRD3*, we examined the influence of the overexpression of clock genes on endogenous mRNA expression levels in C-1300N cells. Although the overexpression of both BMAL1 and CLOCK or D-site-binding protein (DBP) had little effect on the expression of *DRD3*, the overexpression of RORα increased the levels of expression of endogenous *DRD3* mRNA (Fig. 1B). Transactivation of the wild-type (-2427)-Luc reporter by RORα was repressed by cotransfecting with REV-ERBα (Fig. 1C). The transactivation effect of RORα had little effect on the transcriptional activity that was driven by the truncated promoter fragments (Fig. 1D). Incubating wild-type (-2427)-Luc-transfected cells with RORα caused a 3.5-fold increase in promoter activity (Fig. 1E), but this was attenuated by mutation of the ROR response element (RORE).

Role of REV-ERBα in the control of the rhythmic expression of *DRD3* mRNA. Previous studies have demonstrated that several compounds and high concentrations of serum or DEX

Molecular Pharmacology Fast Forward. Published on February 21, 2013 as DOI: 10.1124/mol.112.083535
This article has not been copyedited and formatted. The final version may differ from this version.

are able to induce and/or synchronize circadian gene expression (Balsalobre et al., 2000a; 2000b). Brief exposure of astrocytes to 50% FBS for 2 h induced the rhythmic expression of *DRD3* mRNA (Fig. 2A). We used serum-shocked cells to investigate the role of REV-ERBα on endogenous *DRD3* expression. The treatment of scrambled siRNA (control)-transfected cells with 50% FBS resulted in the induction of significant time-dependent variations in the mRNA levels of *REV-ERBα* ($P < 0.05$, Fig. 2B) and *DRD3* ($P < 0.05$, Fig. 2B); however, no significant time-dependent variations in *DRD3* expression were observed in REV-ERBα-downregulated cells (Fig. 2B, right). In addition, in order to explore the influence of the overexpression of REV-ERBα on the rhythm of expression of DRD3, we tracked the temporal profile of the luciferase activity that was driven by *Drd3::Luc* in C-1300N cells. The control cell exhibited circadian oscillation of reporter bioluminescence driven by *DRD3::Luc* after incubation with DEX. The bioluminescence oscillation that was driven by *DRD3::Luc* in the C-1300N cells was attenuated by transfection with REV-ERBα (Supplemental Fig. 3C).

Time dependency of REV-ERBα binding to the *DRD3* promoter. We determined the 24-h rhythm of the levels of expression of *DRD3* mRNA in the ventral striatum. There was a significant 24-h variation in the mRNA levels of *DRD3* in the ventral striatum, with higher levels during the light phase ($P < 0.01$; cosinor analysis, Fig. 3). Both RORα and REV-ERBα proteins were expressed in the mouse ventral striatum, and they showed a 24-h variation, with a peak

Molecular Pharmacology Fast Forward. Published on February 21, 2013 as DOI: 10.1124/mol.112.083535
This article has not been copyedited and formatted. The final version may differ from this version.

occurring during the dark phase ($P < 0.05$, Fig. 4A; $P < 0.05$, Fig. 4B). However, the fold-change of the protein expression of REV-ERBα at ZT14 was significantly higher than that of RORα at ZT14 (Fig. 4C). This CLOCK-regulated output pathway may be functionally important for the rhythmic expression of *DRD3* mRNA in the ventral striatum. We investigated the temporal binding of endogenous RORα and REV-ERBα protein on the *DRD3* promoter with a ChIP assay. The RORE of the *DRD3* promoter is located between 2231 bp and 2221 bp upstream from the transcription start site. RORα and REV-ERBα that bound to the *DRD3* promoter containing RORE showed a time-dependent variation (Fig. 4D). In addition, the binding levels of REV-ERBα at ZT14 were higher than those of RORα.

Influence of dosing time on the efficacy of 7-OH-DPAT on mouse locomotor activity. We examined the 24-h rhythm of DRD3 protein levels in the mouse ventral striatum. Prior to the analysis of temporal expression profiles of DRD3 protein, we tested the specificity of anti-DRD3 antibody (sc-9114, Santa Cruz Biotechnology), because mature DRD3 protein is thought to be transformed into membrane after glycosylation. The bands of immature DRD3 protein (unglycosylation form) appeared around 50kDa. However, several bands were detected between 50-80 kDa (Supplemental Fig. 1A). The bands detected above 50 kDa seemed to show glycosylation form of DRD3, since the bands were disappeared when the membrane fractions were treated with N-glycosidase (Supplemental Fig. 1B). These results suggest that our used

Molecular Pharmacology Fast Forward. Published on February 21, 2013 as DOI: 10.1124/mol.112.083535
This article has not been copyedited and formatted. The final version may differ from this version.

antibody (sc-9114) can recognize both glycosylation and unglycosylation forms of DRD3 protein. The specificity of the antibody was also confirmed by both immunohistochemical and western blot analysis of NIH3T3 cells that were transfected with human DRD3 expression construct (Supplemental Fig. 1C). The results of western blot analysis revealed that DRD3 protein levels increased during the dark phase (Fig. 5A). Because the expression of DRD3 protein exhibited 24-h rhythm, we tested the influence of the dosing time on the efficacy of 7-OH-DPAT. The compound is a preferential DRD3 agonist and can inhibit locomotor activity. As shown in Fig. 5B, there was a significant dosing time-dependent difference in the activity counts after the 7-OH-DPAT injection. In mice injected with 7-OH-DPAT at ZT14, locomotor activity was decreased at all doses tested (10, 50, and 100 μg/kg; $P < 0.05$). In addition, the effects of 7-OH-DPAT significantly increased in a concentration-dependent manner at ZT14. On the other hands, in the response at ZT2, locomotor activity was decreased with only the high 7-OH-DPAT dose of 100 μg/kg.

Molecular Pharmacology Fast Forward. Published on February 21, 2013 as DOI: 10.1124/mol.112.083535
This article has not been copyedited and formatted. The final version may differ from this version.

Discussion

In this study, we confirmed that the expression of *DRD3* in the mouse ventral striatum was under the control of the molecular organization of the circadian clock. DRD3, which is located in the ventral striatum, modulates dopamine turnover and emotion (Barik et al., 2005). In addition, a recent study demonstrated that the expression of *DRD3* shows a 24-h rhythm (Akhisaroglu et al., 2005). We therefore further focused on the molecular mechanisms underlying the 24-h rhythm of DRD3.

The computer-aided analysis of the mouse *DRD3* promoter identified an E-box element CACGTG, DBP-binding site (D-site) RTTAYGYAAY (R = A or G, Y = C or G), and RORE WWNDAGGTCA (W = A or T, D = A or G or T) sequence approximately 2 kbp upstream of the transcription start site, suggesting that they may potentially serve in the regulation of the expression of the mouse *DRD3* gene by clock genes. We demonstrated that RORα activated the endogenous expression of the *DRD3* gene in C-1300N cells. The results of the analysis with a deleted and mutated DRD3 luciferase reporter construct demonstrated that RORα and REV-ERVα inversely regulated the transcription of the *DRD3* gene through the RORE.

In this study, there was weak effect of the knockdown of REV-ERBα with siRNA on the endogenous expression rhythm of *DRD3* in C1300N cells (Supplemental Fig. 2A). The transduction efficiency of siREV-ERBα in astrocyte cells was higher than in C-1300N cells. The

Molecular Pharmacology Fast Forward. Published on February 21, 2013 as DOI: 10.1124/mol.112.083535
This article has not been copyedited and formatted. The final version may differ from this version.

transfection of the neuroblastoma cell line with lipofection was very difficult. We thus confirmed the expression of DRD3 in astrocytes cells. DRD3 is highly expressed in astrocytes compared to neurons in the striatum (Miyazaki et al., 2004). The expression of DRD3 was decreased in astrocyte cells transfected with siDRD3 (Supplemental Fig. 2A). In addition, the expression of endogenous *DRD3* in astrocyte cells was increased by overexpressed RORα as well as C-1300N cells experiments (Supplemental Fig. 2B). Clock genes were rhythmically expressed in astrocytes (Prolo et al., 2005). Therefore, we used primary astrocytes in this study. The oscillations in the expression of *DRD3* mRNA in serum-shocked cells were modulated by the knockdown of REV-ERBα. Furthermore, the bioluminescence oscillation driven by *Drd3*::*Luc* in the C-1300N cells was diminished by the overexpression of REV-ERBα (Supplemental Fig. 3C). A recent study suggested that REV-ERBα plays a more important role than RORα in the transcriptional circuitry of the clock system. REV-ERBα and RORα regulate the expression of Bmal1 by binding to RORE. REV-ERBα is required for the rhythmic expression of Bmal1, while RORα is dispensable (Liu et al., 2008). In addition, the 24-h rhythm of the expression of *Bmal1* mRNA is blunted in REV-ERBα-mutant mice (Preitner et al., 2002). Taken together, these findings suggest that REV-ERBα participates in the control of the rhythmic expression of *DRD3* mRNA *in vitro*.

The results of the western blot analysis demonstrated that rhythmic patterns of REV-ERBα

Molecular Pharmacology Fast Forward. Published on February 21, 2013 as DOI: 10.1124/mol.112.083535
This article has not been copyedited and formatted. The final version may differ from this version.

protein exhibited time-dependent variations in almost the opposite phase as the *DRD3* mRNA rhythm. The expression of *Bmal1* in the ventral striatum, which is regulated by the expression of REV-ERBα, exhibited not only 24-h variations but also a similar pattern as *DRD3* (Supplemental Fig. 4). These results suggested that the expression of *DRD3* mRNA exhibited a significant circadian rhythm in the ventral striatum. Although the protein expression rhythms of both RORα and REV-ERBα exhibited similar patterns with higher levels from the late light phase to the early dark phase in the ventral striatum and a peak at approximately ZT14, the fold-change of the protein expression of REV-ERBα was larger than that of RORα. Furthermore, the results of the ChIP assay revealed that REV-ERBα bound to the RORE located at 2222–2232 bp in the *DRD3* promoter in a time-dependent manner. The rhythm of the binding of REV-ERBα showed an opposite waveform as that of the expression of *DRD3* mRNA. These results indicated that REV-ERBα is a more important component in the regulation of the rhythmic expression of *DRD3*. These *in vivo* and *in vitro* data suggested that, when the binding amount of REV-ERBα was attenuated, RORα activated the expression of *DRD3* mRNA. As a result, the expression of protein and mRNA of DRD3 exhibited a 24-h rhythm. However, the peak of DRD3 protein was 12 h later than the peak of *DRD3* mRNA in the ventral striatum. Similar findings have been confirmed for different proteins, such as CRY2 and MetAP2 (Lee et al., 2001; Nakagawa et al., 2004). *CRY2* mRNA showed a peak at ZT2, and its protein showed a peak at ZT14. Although the

Molecular Pharmacology Fast Forward. Published on February 21, 2013 as DOI: 10.1124/mol.112.083535
This article has not been copyedited and formatted. The final version may differ from this version.

detailed mechanisms involved are unclear at present, these findings suggested that the degradation process of DRD3 protein requires more time than those of other proteins.

7-OH-DPAT-induced locomotor hypoactivity was more potent in mice injected at ZT14, which corresponded to the peak of the DRD3 protein. Recent studies have demonstrated that the locomotor inhibitory effects of 50 μg/kg and 100 μg/kg doses of 7-OH-DPAT were mediated through DRD2 autoreceptors in DRD3-mutated mice. However, 10 μg/kg did not affect the locomotor inhibition through DRD2, suggesting that low dosage of 7-OH-DPAT more selectively activates DRD3 than DRD2 or other receptors (Pritchard et al., 2003). In addition, 7-OH-DPAT is engaged in activities, such as the inhibition of locomotor activity, without interacting with the 5-HT_{1A} receptor or modulating 5-HT release (Dekeyne et al., 2001). Taken together, because DRD3 protein levels were higher at ZT14, a low 7-OH-DPAT dose (10 μg/kg) may more activate DRD3 than DRD2 and higher dosage (50 μg/kg, 100 μg/kg) activate both DRD2 and DRD3, whereas at ZT2, when DRD3 protein levels are lower, the low dosage of 7-OH-DPAT was without effect on locomotor. These results suggested that the circadian rhythm of DRD3 protein was associated with the dosing time dependence of 7-OH-DPAT-induced locomotor hypoactivity. Futher studies are required to clarify how DRD3 interact to regulate dosing time-dependent change in 7-OH-DPAT-induced locomotor hypoactivity.

In conclusion, this study suggested that RORα and REV-ERBα inversely regulate the

Molecular Pharmacology Fast Forward. Published on February 21, 2013 as DOI: 10.1124/mol.112.083535
This article has not been copyedited and formatted. The final version may differ from this version.

transcription of *DRD3* (Fig. 6). Furthermore, the 24-h rhythm of DRD3 expression is likely to be a mechanism that underlies the time-dependent change in the efficacy of the DRD3 agonist, 7-OH-DPAT. Our present findings revealed that a molecular link between the circadian clock and the function of DRD3 in the ventral striatum acts as a modulator of the pharmacological actions of DRD3 agonists/antagonists.

Molecular Pharmacology Fast Forward. Published on February 21, 2013 as DOI: 10.1124/mol.112.083535
This article has not been copyedited and formatted. The final version may differ from this version.

Acknowledgments

We are also grateful to Mr. Yasuhiko Hayakawa and Mr. Kazunori Hirakawa (NEPAGENECO.LTD, Japan) for the technical support of transfection to the cells by electroporation using Super Electroporator NEPA21 (NEPA GENE, Co. Ltd, Ichikawa, Japan).

Molecular Pharmacology Fast Forward. Published on February 21, 2013 as DOI: 10.1124/mol.112.083535
This article has not been copyedited and formatted. The final version may differ from this version.

Authorship contributions

Participated in research design: Ikeda, Matsunaga, Koyanagi, Ohdo.

Conducted experiments: Ikeda, Matsunaga, Kakimoto.

Contributed new reagents or analysis: Ikeda, Kakimoto, Hamamura, Hayashi.

Performed date analysis: Ikeda, Kakimoto, Koyanagi.

Wrote or contributed to the writing of the manuscript: Ikeda, Matsunaga, Ohdo.

References

Akhisaroglu M, Kurtuncu M, Manev H, and Uz T. (2005) Diurnal rhythms in quinpirole-induced locomotor behaviors and striatal D2/D3 receptor levels in mice. *Pharmacol Biochem Behav.* 80: 371-377.

Balsalobre A, Marcacci L, and Schibler U. (2000a) Multiple signaling pathways elicit circadian gene expression in cultured Rat-1 fibroblasts. *Curr Biol* 10: 1291-1294.

Balsalobre A, Brown SA, Marcacci L, Tronche F, Kellendonk C, Reichardt HM, Schütz G and Schibler U. (2000b) Resetting of circadian time in peripheral tissues by glucocorticoid signaling. *Science* 289: 2344-2347.

Barik S, de Beaurepaire R. (2005) Dopamine D3 modulation of locomotor activity and sleep in the nucleus accumbens and in lobules 9 and 10 of the cerebellum in the rat. *Prog Neuropsychopharmacol Biol Psychiatry* 29: 718-726.

Bézard E, Ferry S, Mach U, Stark H, Leriche L, Boraud T, Gross C and Sokoloff P. (2003) Attenuation of levodopa-induced dyskinesia by normalizing dopamine D3 receptor function. *Nat Med.* 9: 762-767.

Boulay D, Depoortere R, Perrault G, Borrelli E, and Sanger DJ. (1999) Dopamine D2 receptor knock-out mice are insensitive to the hypolocomotor and hypothermic effects of dopamine D2/D3 receptor agonists. *Neuropharmacology.* 38: 1389-1396.

Bouthenet ML, Souil E, Martres MP, Sokoloff P, Giros B, and Schwartz JC. (1991). Localization of dopamine D3 receptor mRNA in the rat brain using in situ hybridization histochemistry: comparison with dopamine D2 receptor mRNA. *Brain Res.* 564: 203-219.

Bugge A, Feng D, Everett LJ, Briggs ER, Mullican SE, Wang F, Jager J, and Lazar MA. (2012) Rev-erbα and Rev-erbβ coordinately protect the circadian clock and normal metabolic function. *Genes Dev.* 26: 657-667.

Civelli O, Bunzow JR, and Grandy DK. (1993) Molecular diversity of the dopamine receptors. *Annu Rev Pharmacol Toxicol.* 33: 281-307.

Dekeyne A, Rivet JM, Gobert A, and Millan MJ. (2001) Generalization of serotonin $(5\text{-HT})_{1A}$ agonists and the antipsychotics, clozapine, zipradone and S16924, but not haloperidol, to the discriminative stimuli elicited by PD128,907 and 7-OH-DPAT. *Neuropharmacology* 40: 899-910.

Diaz J, Pilon C, Le Foll B, Gros C, Triller A, Schwartz JC, and Sokoloff P. (2000) Dopamine D3 receptors expressed by all mesencephalic dopamine neurons. *J Neurosci.* 20: 8677-8684

Everett PB, Senogles SE. (2010) D3 dopamine receptor signals to activation of phospholipase D through a complex with Rho. *J Neurochem.* 112: 963-971.

Franklin, K.J, and Paxinos, G. (1997) *The Mouse Brain in Stereotaxic Coordinates. Academic Press,* San Diego.

Gekakis N, Staknis D, Nguyen HB, Davis FC, Wilsbacher LD, King DP, Takahashi JS, and Weitz

CJ. (1998) Role of the CLOCK protein in the mammalian circadian mechanism. *Science* 280: 1564-1569.

Gingrich JA, and Caron MG. (1993) Recent advances in the molecular biology of dopamine receptors. *Annu Rev Neurosci.* 16: 299-321.

Gurevich EV, Bordelon Y, Shapiro RM, Arnold SE, Gur RE and Joyce JN. (1997) Mesolimbic dopamine D3 receptors and use of antipsychotics in patients with schizophrenia. A postmortem study. *Arch Gen Psychiatry.* 54: 225-232.

Hashiramoto A, Yamane T, Tsumiyama K, Yoshida K, Komai K, Yamada H, Yamazaki F, Doi M, Okamura H, and Shiozawa S. (2010) Mammalian clock gene Cryptochrome regulates arthritis via proinflammatory cytokine TNF-alpha. *J Immunol* 184: 1560-1565.

Ishida A, Mutoh T, Ueyama T, Bando H, Masubuchi S, Nakahara D, Tsujimoto G, and Okamura H. (2005) Light activates the adrenal gland: timing of gene expression and glucocorticoid release. *Cell Metab* 2: 297-307.

Jin X, Shearman LP, Weaver DR, Zylka MJ, de Vries GJ, and Reppert SM. (1999) A molecular mechanism regulating rhythmic output from the suprachiasmatic circadian clock. *Cell* 96: 57-68.

Joyce JN. (2001) Dopamine D3 receptor as a therapeutic target for antipsychotic and antiparkinsonian drugs. *Pharmacol Ther.* 90: 231-259.

Kume K, Zylka MJ, Sriram S, Shearman LP, Weaver DR Jin X, Maywood ES, Hastings MH, and

Reppert SM. (1999) mCRY1 and mCRY2 are essential components of the negative limb of the circadian clock feedback loop. *Cell* 98: 193-205.

Lee C, Etchegaray JP, Cagampang FR, Loudon AS,and Reppert SM. (2001) Posttranslational mechanisms regulate the mammalian circadian clock. *Cell* 107: 855-867.

Liu AC, Tran HG, Zhang EE, Priest AA, Welsh DK, and Kay SA. (2008) Redundant function of REV-ERBalpha and beta and non-essential role for Bmal1 cycling in transcriptional regulation of intracellular circadian rhythms. *PLoS Genet.* 4: e1000023.

Matsuo T, Yamaguchi S, Mitsui S, Emi A, Shimoda F, and Okamura H. (2003) Control mechanism of the circadian clock for timing of cell division in vivo. *Science* 302: 255-259.

Missale C, Nash SR, Robinson SW, Jaber M, and Caron MG. (1998) Dopamine receptors: from structure to function. *Physiol Rev.* 78: 189-225.

Miyazaki I, Asanuma M, Diaz-Corrales FJ, Miyoshi K, Ogawa N. (2004) Direct evidence for expression of dopamine receptors in astrocytes from basal ganglia. *Brain Res.* 1029: 120-123.

Nakagawa H, Koyanagi S, Takiguchi T, Kuramoto Y, Soeda S, Shimeno H, Higuchi S, and Ohdo S. (2004) 24-hour oscillation of mouse methionine aminopeptidase2, a regulator of tumor progression, is regulated by clock gene proteins. *Cancer Res*. 64: 8328-8333.

Oishi K, Miyazaki K, Kadota K, Kikuno R, Nagase T, Atumi G, Ohkura N, Azama T, Mesaki M, Yukimasa S, et al. (2003) Genome-wide expression analysis of mouse liver reveals

CLOCK-regulated circadian output genes. *J Biol Chem.* 278: 41519-41527.

Ohdo S, Koyanagi S, Matsunaga N, and Hamdan A. (2011) Molecular basis of chronophamaceutics. *J Pharmaceutics Science* 100: 3560-3573.

Ozaki N, Noshiro M, Kawamoto T, Nakashima A, Honda K, Fukuzaki-Dohi U, Honma S, Fujimoto K, Tanimoto K, Tanne K, and Kato Y. (2012) Regulation of basic helix-loop-helix transcription factors *Dec1* and *Dec2* by RORα and their roles in adipogenesis. *Genes Cells* 17: 109-121.

Paul P, Etienne C. (2011) Melatonin: Both master clock output and internal time-giver in the circadian clocks network. *J Physiology* 105: 170-182.

Prolo LM, Takahashi JS, and Herzog ED. (2005) Circadian rhythm generation and entrainment in astrocytes. *J Neurosci.* 25: 404-408.

Preitner N, Damiola F, Lopez-Molina L, Zakany J, Duboule D, Albrecht U, and Schibler U. (2002) The orphan nuclear receptor REV-ERBalpha controls circadian transcription within the positive limb of the mammalian circadian oscillator. *Cell* 110: 251-60.

Pritchard LM, Logue AD, Hayes S, Welge JA, Xu M, Zhang J, Berger SP, and Richtand NM. (2003) 7-OH-DPAT and PD 128907 selectively activate the D3 dopamine receptor in a novel environment. *Neuropsychopharmacology* 28: 100-107.

Reuss B, Dermietzel R, and Unsicker K. (1998) Fibroblast growth factor 2 (FGF-2) differentially

regulates connexin (cx) 43 expression and function in astroglial cells from distinct brain regions. *GLIA* 22: 19-30

Shimba S, Ishii N, Ohta Y, Ohno T, Watabe Y, Hayashi M, Wada T, Aoyagi T, and Tezuka M. (2005) Brain and muscle Arnt-like protein-1 (BMAL1), a component of the molecular clock, regulates adipogenesis. *Proc Natl Acad Sci USA*. 102: 12071-12076.

Xu M, Koeltzow TE, Santiago GT, Moratalla R, Cooper DC, Hu XT, White NM, Graybiel AM, White FJ, and Tonegawa S. (1997) Dopamine D3 receptor mutant mice exhibit increased behavioral sensitivity to concurrent stimulation of D1 and D2 receptors. *Neuron* 19: 837-848.

Footnotes

This study was supported partially by the Ministry of Education, Culture, Sport, Science and Technology [Grants-in-Aid for Scientific Research on Priority Areas “Cancer” 20014016]; a Grant-in-Aid for Scientific Research (B) [Grant 1390047]; the Japan Society for the Promotion of Science [Grant-in-Aid for Challenging Exploratory Research 21659041]; and a Grant-in-Aid for the Encouragement of Young Scientists [Grant 24590196] from the Japan Society for the Promotion of Science.

E.I. and N.M. contributed equally to this work.

Molecular Pharmacology Fast Forward. Published on February 21, 2013 as DOI: 10.1124/mol.112.083535
This article has not been copyedited and formatted. The final version may differ from this version.

Legends for Figures

Figure 1. Transcriptional regulation of the *DRD3* gene by clock genes. (A) Schematic representation of the mouse *DRD3* promoter. The numbers below the boxes are the nucleotide residues in which the retinoic acid-related orphan receptor α (RORα) response element (RORE), the E-box, and the D-site are positioned relative to the transcription start site (+1). The underlined nucleotide residues indicate the mutated sequence of the RORE. (B) Transcriptional regulation of endogenous *DRD3* mRNA by clock genes. C-1300N cells were transfected with expression plasmids (2 μg each of RORα, BMAL1, CLOCK, and DBP). Each value is presented as the mean ± standard error of the mean (S.E.; n = 6). *, $P < 0.05$ compared to pcDNA3.1. (C) Transcriptional regulation of the *DRD3* promoter [Wild-type (2427)-Luc] by RORα and REV-ERBα. The presence (+) or absence (-) of plasmids (0.1 μg of wild-type-Luc; 1 μg of each of RORα and REV-ERBα) is noted. Each value is presented as the mean ± S.E. (n = 3). *, $P < 0.05$ compared to nontreated wild-type (2427)-Luc. (D) Transcriptional regulation of the deleted *DRD3* promoter by RORα and REV-ERBα. Astrocytes were transfected with 1 μg each of RORα and REV-ERBα. Each value is presented as the mean ± S.E. (n = 3–9). *, $P < 0.05$ compared to pcDNA3.1. (E) Mutation of RORE abrogates the RORα-induced *DRD3* promoter activity. The presence (+) or absence (-) of plasmids (0.1 μg for each of wild-type-Luc and RORE mut-Luc; 1 μg of RORα) is noted. Each value is presented as the mean ± S.E. (n = 3). *, $P < 0.05$ compared

Molecular Pharmacology Fast Forward. Published on February 21, 2013 as DOI: 10.1124/mol.112.083535
This article has not been copyedited and formatted. The final version may differ from this version.

to nontreated wild-type (2427)-Luc. #, P < 0.05 compared to RORα-transfected wild-type-Luc.

Figure 2. REV-ERBα is required for the circadian transcription of *DRD3* mRNA. (A) Temporal mRNA expression profile of DRD3 in astrocytes after serum treatment. Each value is presented as the mean ± S.E. (n = 3). (B) The influence of the downregulation of REV-ERBα on the oscillation of the expression of REV-ERBα and *DRD3* mRNA. Astrocytes were transfected with scrambled siRNA (Control siRNA) or specific siRNA for REV-ERBα (REV-ERBα siRNA). Transfected cells were treated with 50% fetal bovine serum for 2 h and subsequently incubated in serum-starved medium. The mRNA levels of *DRD3* were determined from 24 h to 52 h after serum treatment. ●, Control siRNA; ○, REV-ERBα siRNA; each value is presented as the mean ± S.E. (n = 3) (control siRNA; P < 0.05, cosinor analysis).

Figure 3. Twenty-four-hour rhythm of the mRNA levels of *DRD3* in the ventral striatum. The temporal profiles of *DRD3* mRNA in the ventral striatum. The mean peak value was set at 100%. Each value is presented as the mean ± S.E. (n = 3) (P < 0.01, cosinor analysis).

Figure 4. Temporal profile of endogenous REV-ERBα binding to the *DRD3* in the ventral striatum. (A,B) Temporal expression profile of RORα and REV-ERBα proteins in the ventral striatum. Nuclear proteins were probed by western blot analyses with antibodies against RORα, REV-ERBα, and polymerase 2. Each value is presented as the mean ± S.E. (n = 3–5) (RORα and REV-ERBα; P < 0.05, cosinor analysis). (C) Fold changes in the RORα and REV-ERBα

Molecular Pharmacology Fast Forward. Published on February 21, 2013 as DOI: 10.1124/mol.112.083535
This article has not been copyedited and formatted. The final version may differ from this version.

protein levels in the ventral striatum at Zeitgerber time (ZT)2 or ZT14. Each value is presented as the mean ± S.E. (n = 3–5). *, P < 0.05 compared to REV-ERBα protein at ZT2. #, P < 0.05 compared to REV-ERBα protein at ZT14. (D) Chromatin immunoprecipitation analysis of the *DRD3* promoter in the ventral striatum. The photographs show representative electrophoretic images of the polymerase chain reaction (PCR) products of RORα, REV-ERBα, IgG binding, and input DNA. The graph shows the relative PCR values (P < 0.05 for all, cosinor analysis). Each value is presented as the mean ± S.E. (n = 3). *, P < 0.05 compared to RORα at corresponding ZTs.

Figure 5. Influence of dosing time on the efficacy of 7-hydroxy-*N*,*N*-dipropyl-2-aminotetralin (7-OH-DPAT) on mouse locomotor activity. (A) Temporal expression profiles of DRD3 protein in the ventral striatum. Left photographs show representative western blots of image DRD3 protein in ventral striatum. Protein levels were revealed by the analysis of surrounding bands signal of the 75kDa (a), 63kDa (b) or 48kDa (c). β-actin protein was used as an internal control. The mean peak value was set at 100%. Each value is presented as the mean ± S.E. (n = 3) (75kDa; P<0.05, 63kDa; P=0.11, 43kDa; P = 0.057, cosinor analysis). **, P < 0.01 compared to ZT2. (B) Influence of the dosing time on the efficacy of 7-OH-DPAT on mouse locomotor activity. Thirty-min activity counts were assessed after the injection of 7-OH-DPAT (10, 50, or 100 μg/kg, i.p.) at ZT2 or ZT14. Each column represents the

Molecular Pharmacology Fast Forward. Published on February 21, 2013 as DOI: 10.1124/mol.112.083535
This article has not been copyedited and formatted. The final version may differ from this version.

mean ± S.E. (n = 3). *, P < 0.05 compared to the vehicle-treated group at the corresponding time.

Figure 6. Molecular mechanisms underlying the 24-h variations in the expression of DRD3 in the ventral striatum. The regulation of the expression of the *DRD3* gene by RORα and REV-ERBα in the ventral striatum. The expression of RORα and REV-ERBα is governed by central components of the circadian oscillator; the expression of these genes fluctuates in almost the same phase. RORα activates the transcription of the *DRD3* gene, whereas REV-ERBα periodically suppresses transcription when REV-ERBα is abundant. As a result, RORα and REV-ERBα control the amplitude of the rhythm in DRD3 expression.

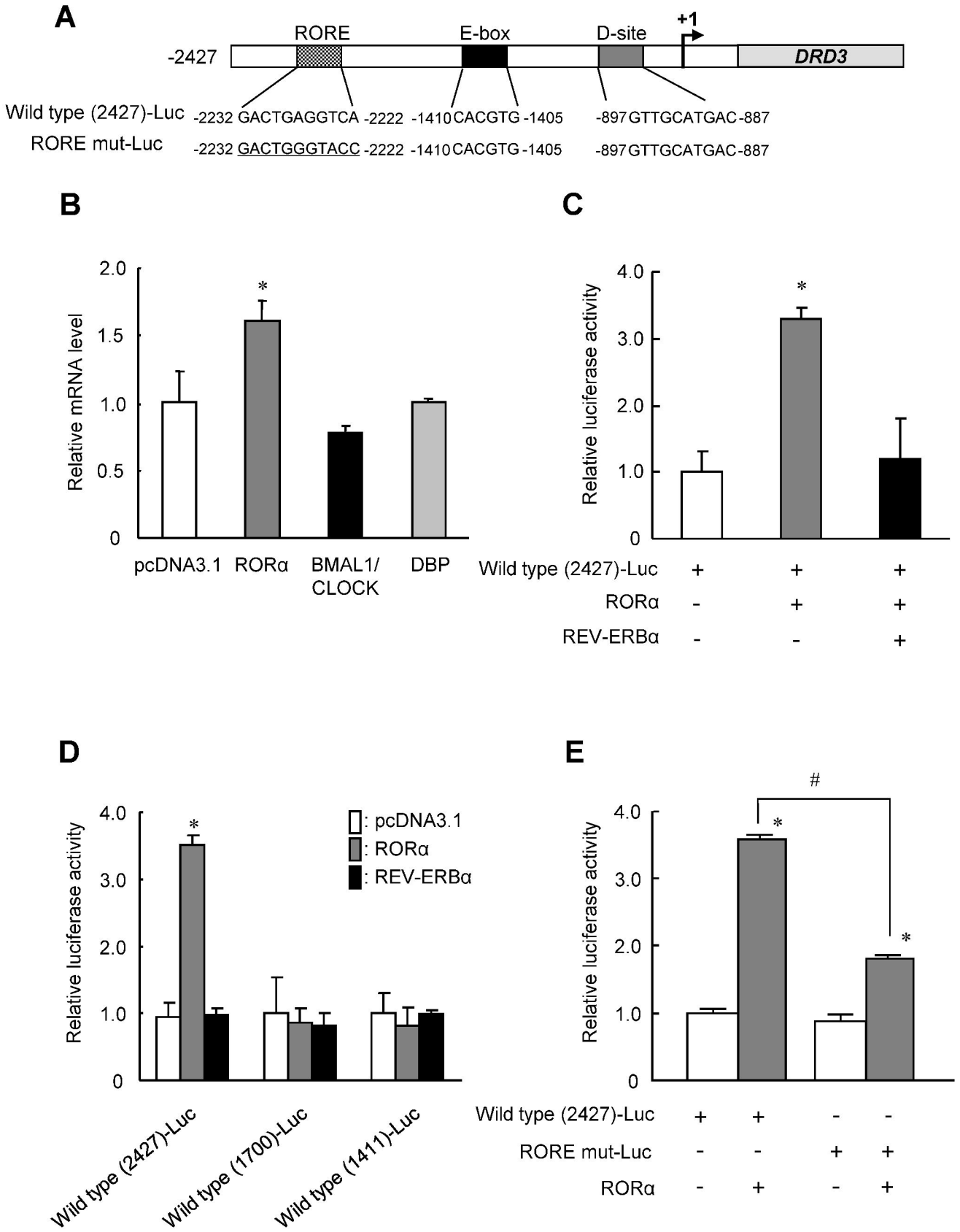
A
RORE
E-box
D-site
+1
-2427
DRD3
Wild type (2427)-Luc
-2232 GACTGAGGTCA -2222
-1410 CACGTG -1405
-897 GTTGCATGAC -887
RORE mut-Luc
-2232 GACTGGGTACC -2222
-1410 CACGTG -1405
-897 GTTGCATGAC -887
B
Relative mRNA level
2.0
1.5
1.0
0.5
0
*
pcDNA3.1
RORα
BMAL1/ CLOCK
DBP
C
Relative luciferase activity
4.0
3.0
2.0
1.0
0
*
Wild type (2427)-Luc + + +
RORα - + +
REV-ERBα - - +
D
Relative luciferase activity
4.0
3.0
2.0
1.0
0
*
: pcDNA3.1
: RORα
: REV-ERBα
Wild type (2427)-Luc
Wild type (1700)-Luc
Wild type (1411)-Luc
E
Relative luciferase activity
4.0
3.0
2.0
1.0
0
#
*
*
Wild type (2427)-Luc + + - -
RORE mut-Luc - - + +
RORα - + - +

Figure 1

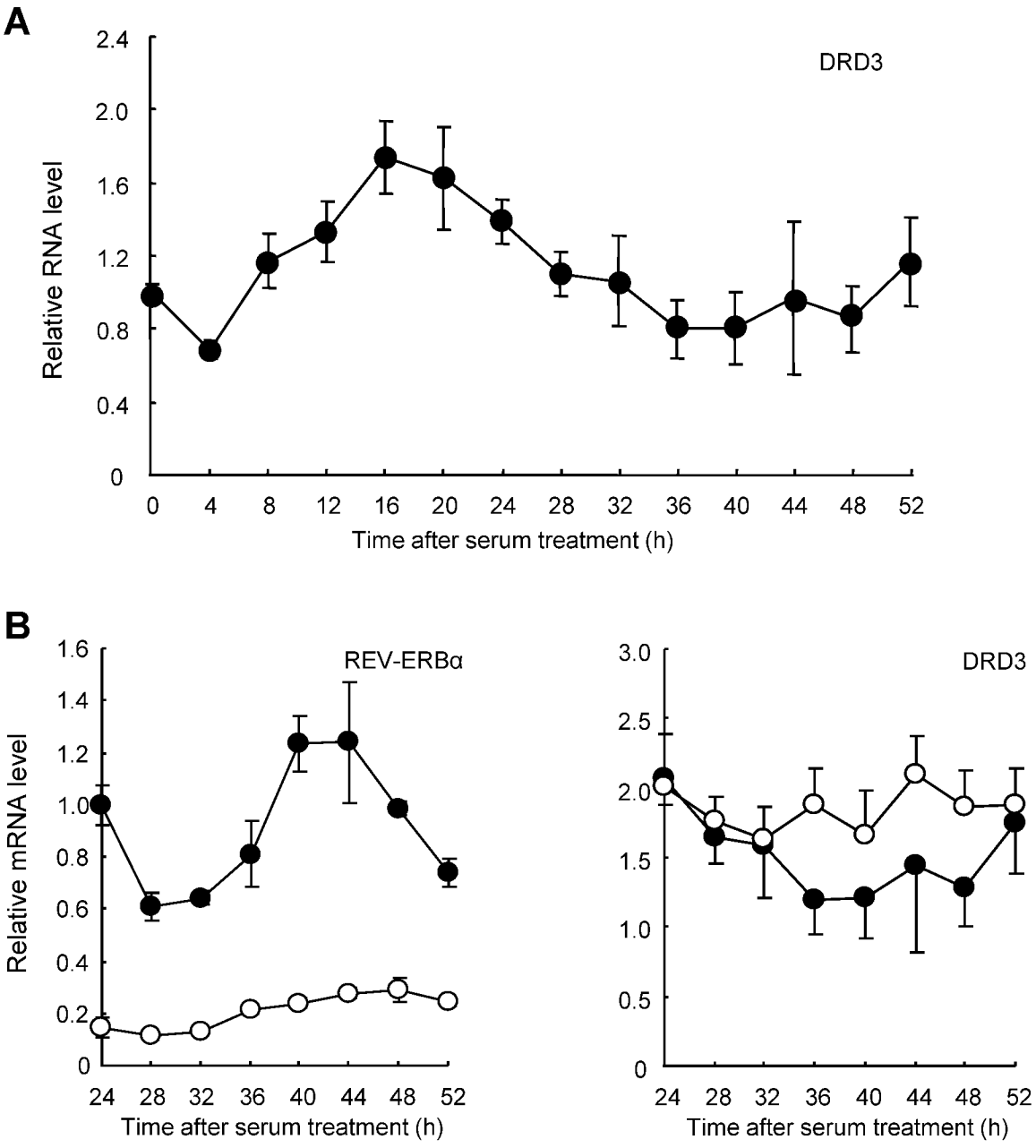
A
DRD3
Relative RNA level
2.4
2.0
1.6
1.2
0.8
0.4
0
0 4 8 12 16 20 24 28 32 36 40 44 48 52
Time after serum treatment (h)
B
REV-ERBα
Relative mRNA level
1.6
1.4
1.2
1.0
0.8
0.6
0.4
0.2
0
24 28 32 36 40 44 48 52
Time after serum treatment (h)
DRD3
3.0
2.5
2.0
1.5
1.0
0.5
0
24 28 32 36 40 44 48 52
Time after serum treatment (h)

Figure 2

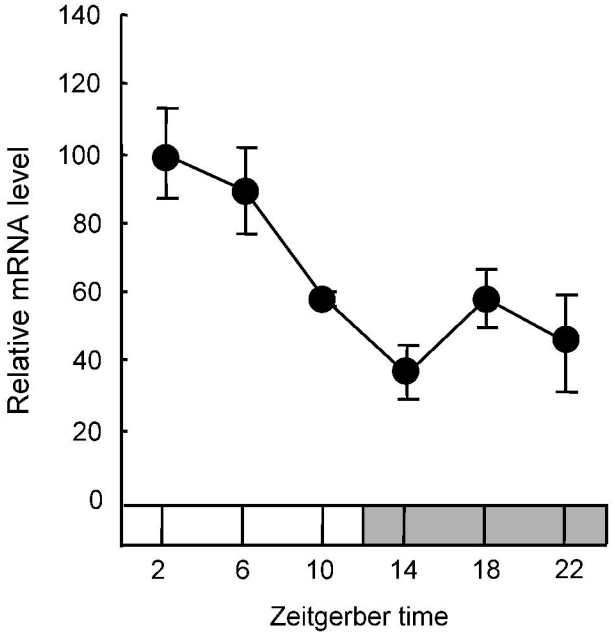
140
120
100
80
60
40
20
0
Relative mRNA level
2
6
10
14
18
22
Zeitgerber time

Figure 3

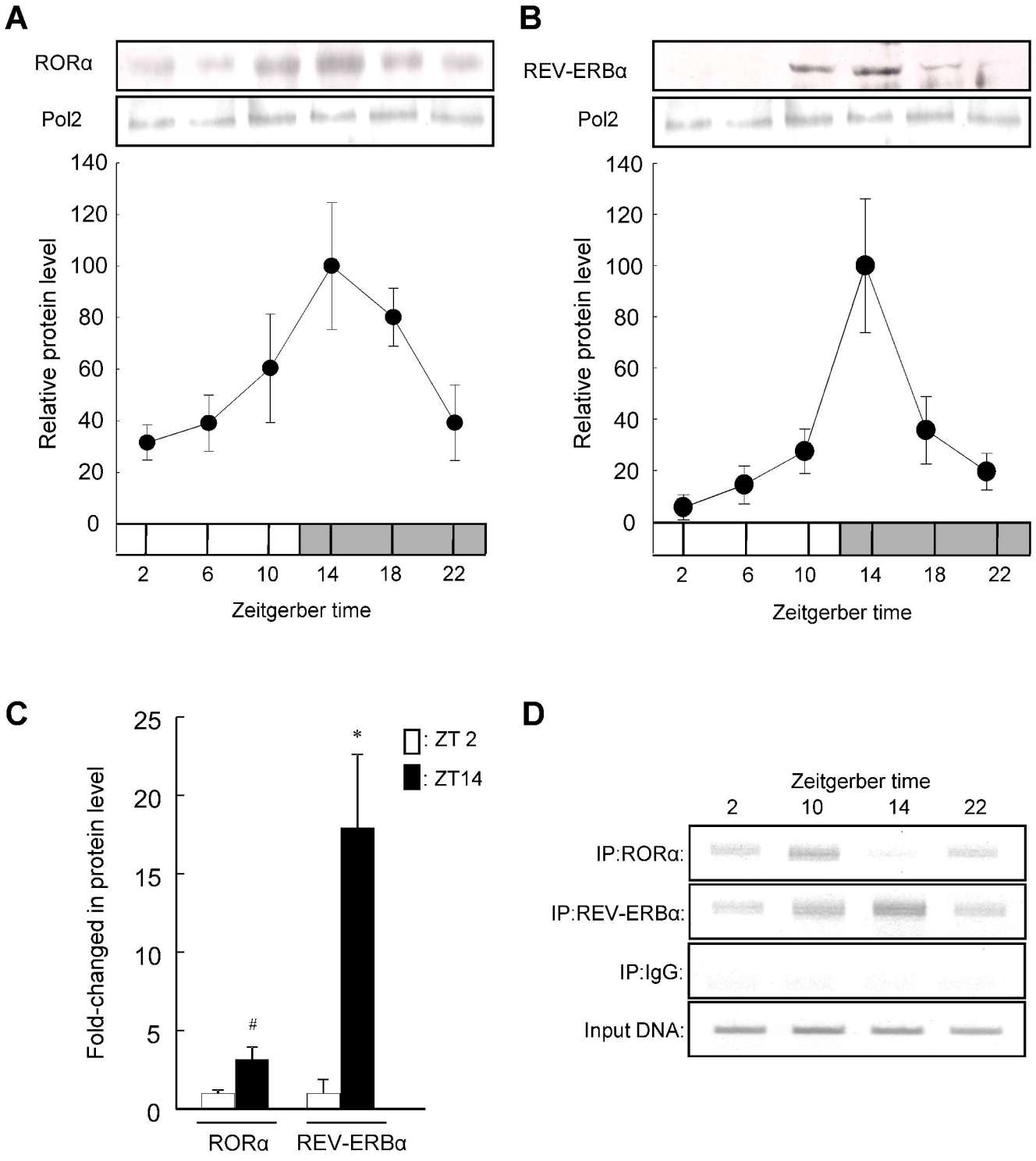
A
RORα
Pol2
Relative protein level
140
120
100
80
60
40
20
0
2
6
10
14
18
22
Zeitgerber time
B
REV-ERBα
Pol2
Relative protein level
Zeitgerber time
C
Fold-changed in protein level
25
20
15
10
5
0
*
#
: ZT 2
: ZT14
RORα
REV-ERBα
D
Zeitgerber time
2
10
14
22
IP:RORα:
IP:REV-ERBα:
IP:IgG:
Input DNA:

Figure 4

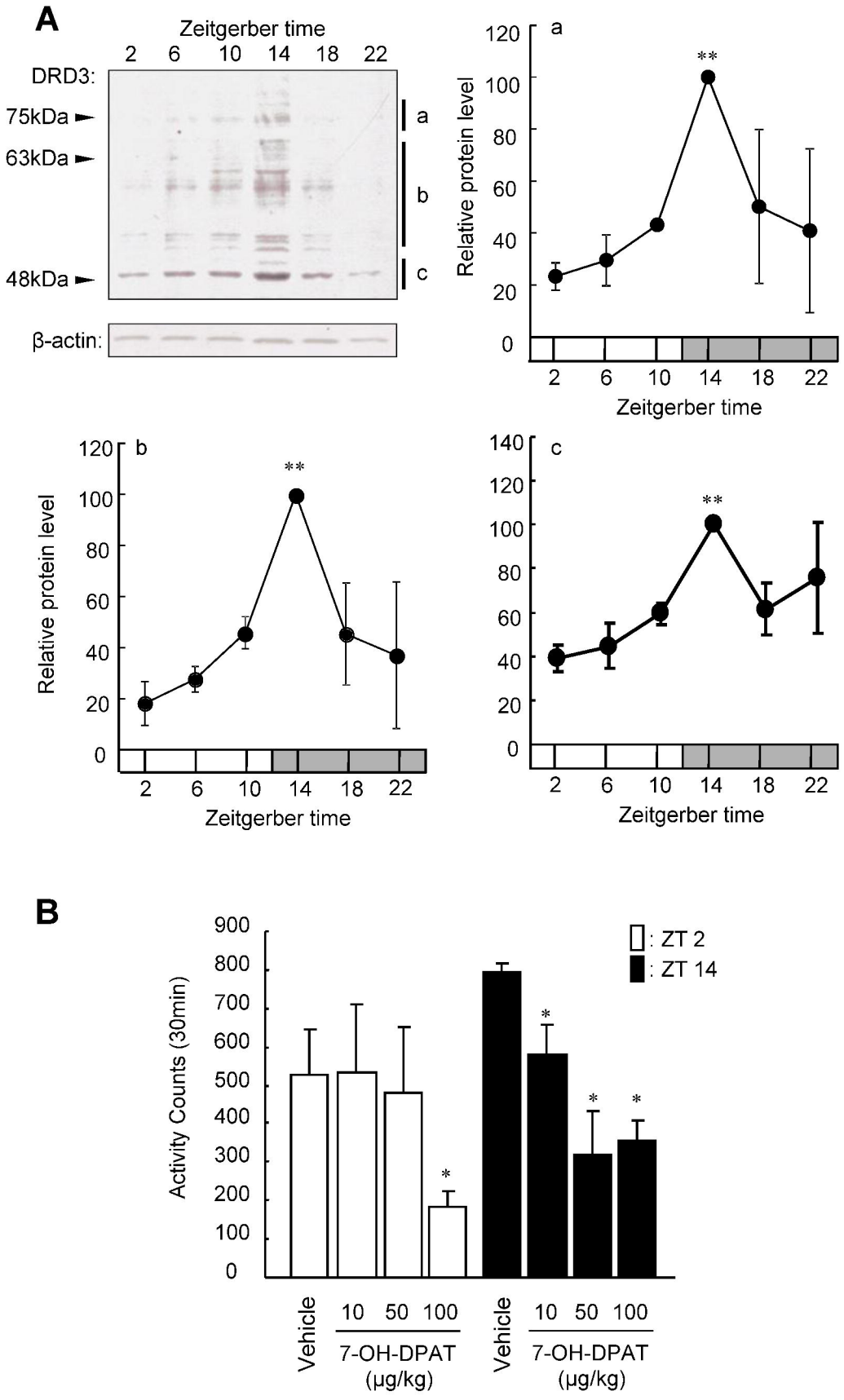
A
Zeitgerber time
2 6 10 14 18 22
DRD3:
75kDa
63kDa
48kDa
β-actin:
a
b
c
Relative protein level
Zeitgerber time
**
B
Activity Counts (30min)
: ZT 2
: ZT 14
*
Vehicle
10 50 100
7-OH-DPAT
(μg/kg)

Figure 5

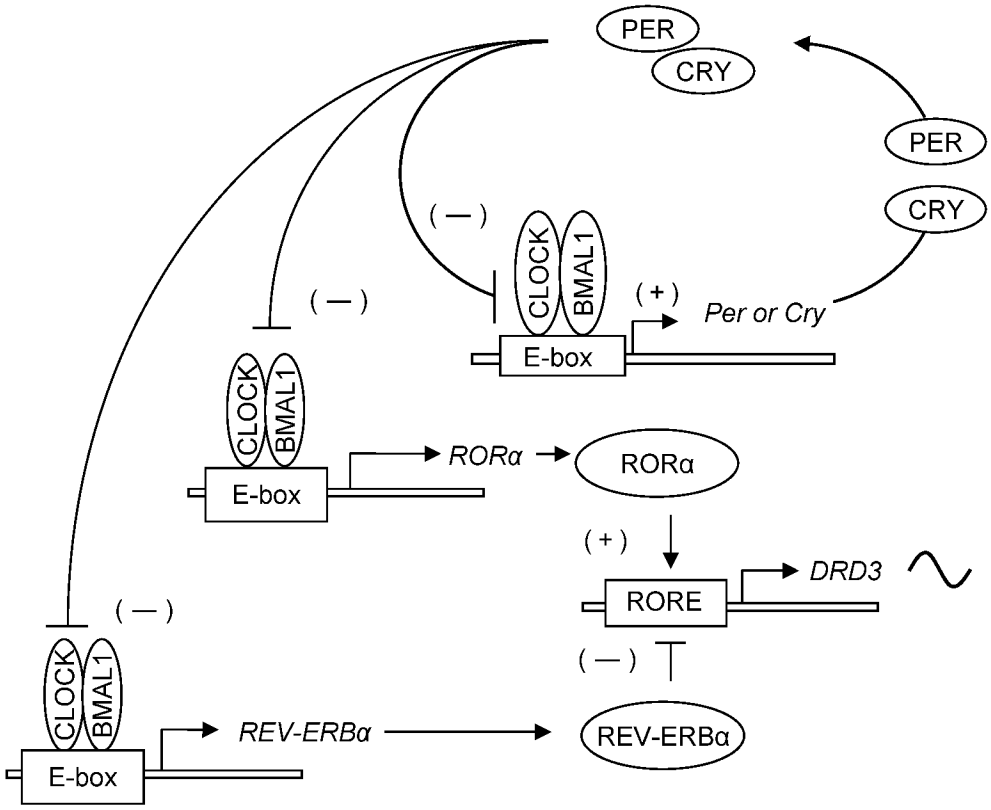
PER
CRY
PER
CRY
(—)
CLOCK
BMAL1
(+)
Per or Cry
E-box
(—)
CLOCK
BMAL1
E-box
RORα
RORα
(+)
DRD3
RORE
(—)
(—)
CLOCK
BMAL1
E-box
REV-ERBα
REV-ERBα

Figure 6

in vitro electroporation

The cell suspension ($1X10^6$ cells) was mixed with plasmid 1 μg pcDNA3.1 intact vector or pcDNA3.1 human drd3 in Opti-MEM™ Media (GIBCO). The expression plasmid of pcDNA3.1 was obtained by Missouri S&T cDNA Resource Center. The cell and plasmid suspension was then transferred to a cuvette, and the plasmids were transferred to the cells by electroporation using Super Electroporator NEPA21 (NEPA GENE, Co. Ltd, Ichikawa, Japan). Square electric pulses were applied at 150 V (pulse length, 0.5 ms; two pulses; interval, 50 ms), followed by additional pulses at 20 V (pulse length, 50 ms; five pulses; interval, 50 ms).

Cell culture and immunocytochemistry

The transfected cells were cultured in the same medium for 2 days in vitro. The cells were then fixed with 4% paraformaldehyde in phosphate-buffered saline (PBS) for 10 min at room temperature (RT). Subsequently, cells were treated with PBS containing 3% Bovine Albumin (BSA) for 1 h at RT. This was followed by incubation in the primary antibody diluted in PBS with 0.1% BSA for 2 h at overnight at 4 °C. The primary antibodies used were as follows: rabbit anti-DRD3 (1 : 250; Santa Cruz Biotechnology). The sections were incubated for 1 h at RT in the secondary antibody diluted in PBS with 0.1% BSA. The secondary antibodies used were as follows: Cy3 anti-rabbit (1 : 1000; Sigma–Aldrich, St. Louis, MO). Photographs were taken with a fluorescence microscope (Biozero BZ-9000 Keyence).

Deglycosylation Assay

Protein samples were incubated with *N*-glycosidase F for 17 h at 37°C according to the supplier's instructions (TaKaRa Bio Inc.). We used 1mU *N*-glycosidase F per 25 μg of glycoprotein. Controls were incubated without enzyme. Analysis was carried out by 8 % SDS_PAGE under reducing conditions, and immunoblots were revealed by DRD3 antibody (Santa Cruz).

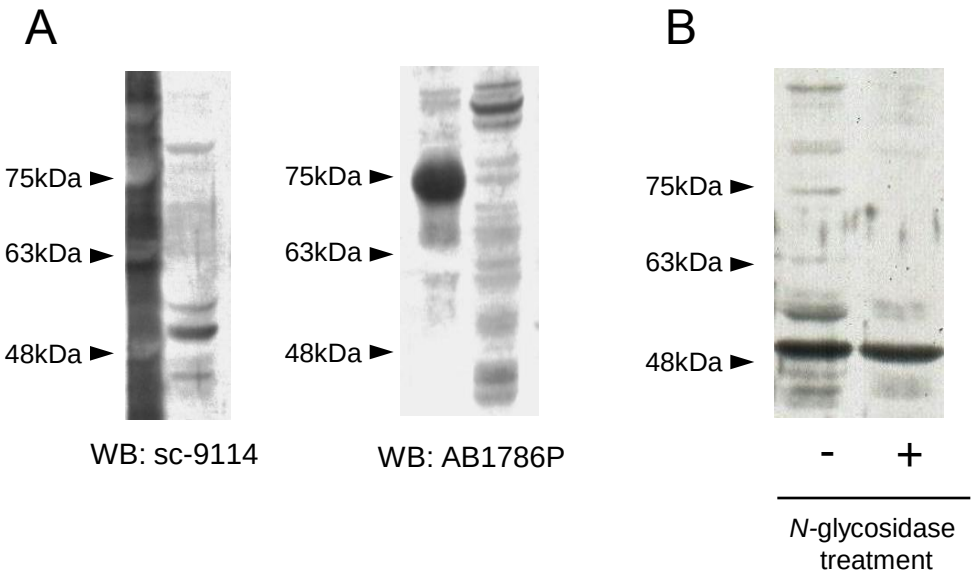

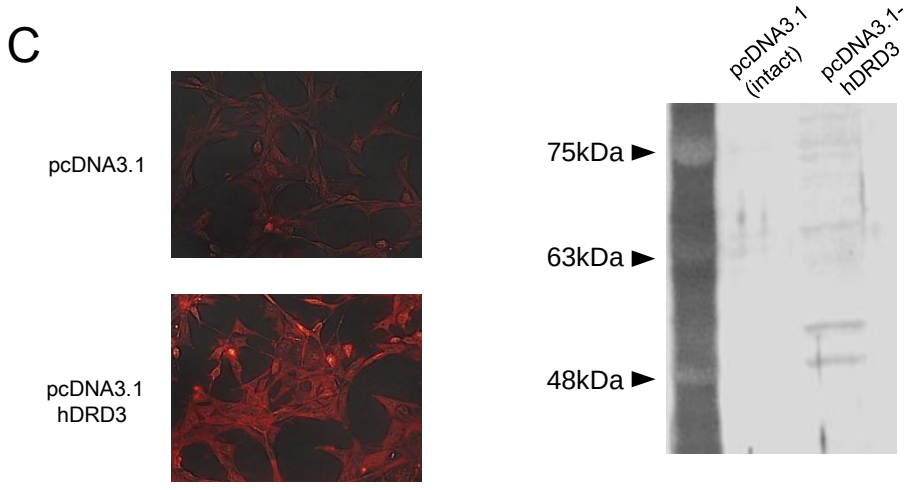

Supplemental Figure 1 Recognition of both glycosylation and unglycosylation forms of DRD3 protein by anti-DRD3 antibody (sc-9114). (A) Representative photographs of western blot analysis for DRD3 protein in ventral striatum of mice using two different antibodies, sc-9114 (left) and AB1786P (right). The band around 50kDa reveals immature DRD3 protein. Several bands above 50kDa indicate glycosylation form of DRD3 protein. Data shown were confirmed in three independent experiments. (B) Representative photographs of western blot analysis for DRD3 protein in ventral striatum of mice after treatment with *N*-glycosidase. Protein samples prepared form ventral striatum of mice were treated with *N*-glycosidase (Takara Bio Inc.) at 37 ^{o}C for 17 h. The digested protein samples were subjected to western blot analysis using anti-DRD3 antibody (sc-9114). Data shown were confirmed in three independent experiments. (C) Representative photographs of immunohistochemical (left) and western blot (right) analyzes for DRD3 protein in NIH3T3 cells transfected with human DRD3 expression constructs or pcDNA 3.1 empty vectors. Data shown were confirmed in three independent experiments.

Supplemental Figure 1

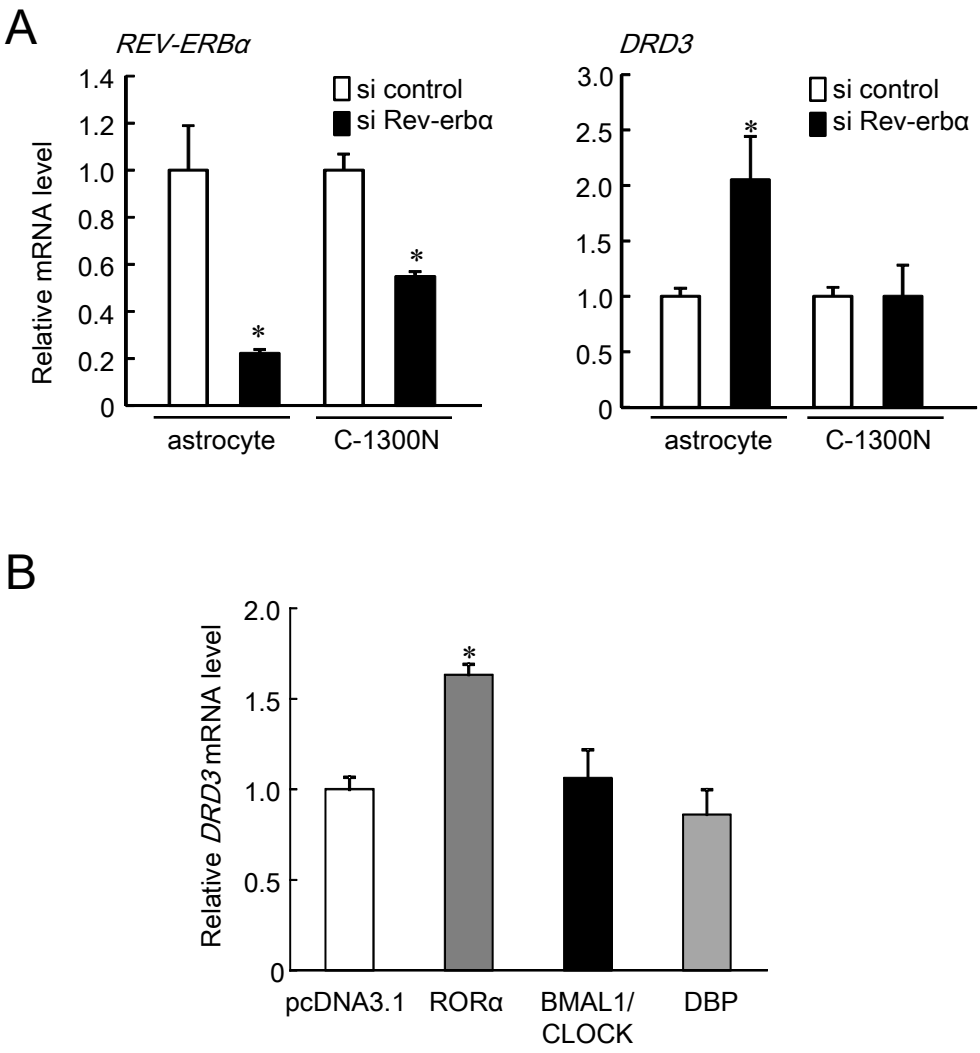

Supplemental Figure 2 Influence of siDRD3 on expression of DRD3 in astrocyte cell. (A)The expression level of *REV-ERBα or DRD3* mRNA in siRNA transfected astrocyte or C-1300N cell at 44 hr after serum shocked. Each value is the mean ± S.E. (n=3). *; P<0.05 compared with si control. (B) Transcriptional regulation of endogenous *DRD3* mRNA by clock genes. Astrocytes were transfected with expression plasmids (2 μg; each of RORα, BMAL1, CLOCK and DBP). Each value is the mean ± S.E. (n=3). *; P<0.05 compared with pcDNA.

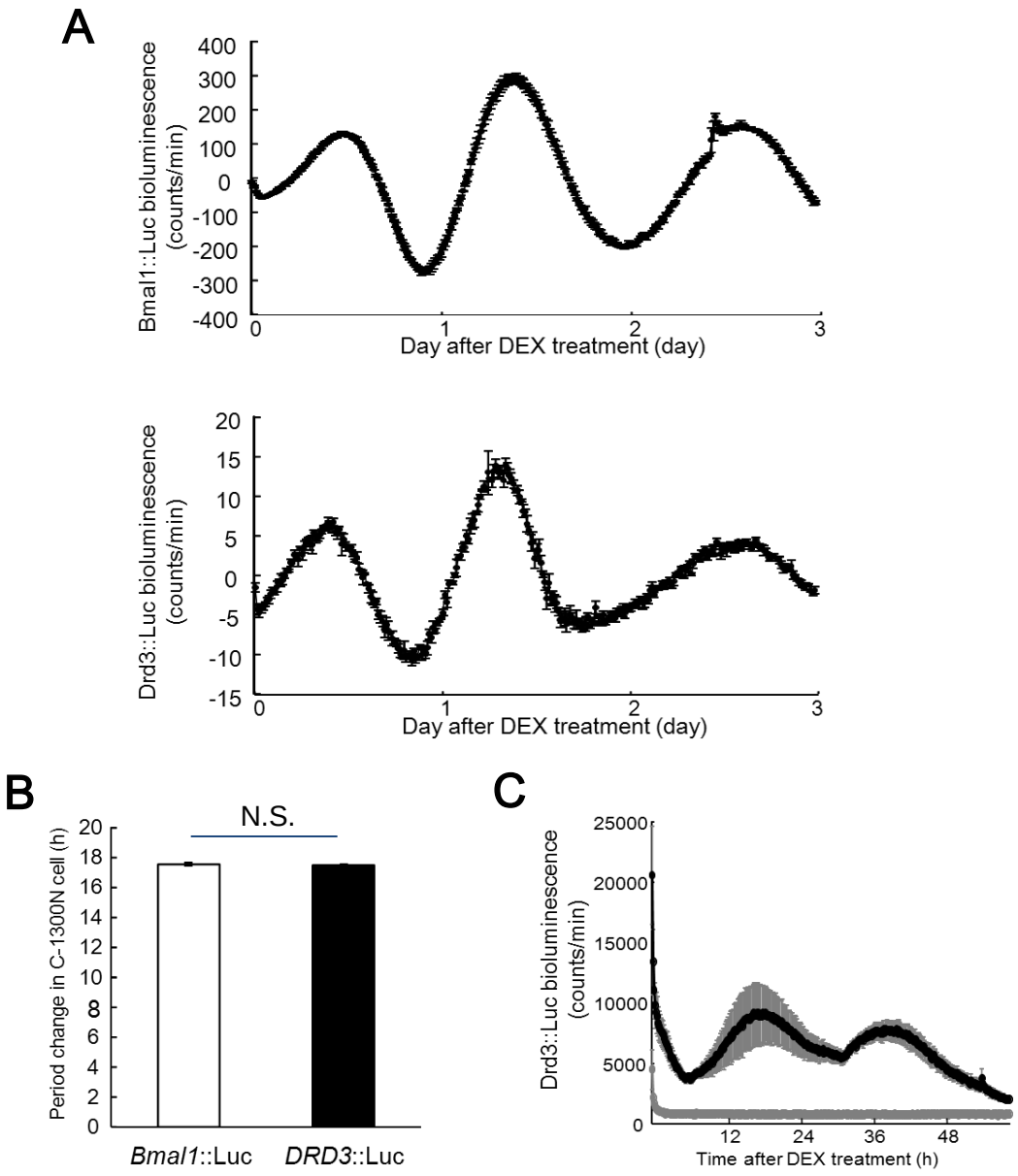

Supplemental Figure 3 Influence of REV-ERBα on circadian oscillation. (A) Upper panel: Representative traces of bioluminescent oscillations driven by *Bmal1::luc* in C-1300N cells with the lumicycle (neuroscience). Lower panel: Representative traces of bioluminescent oscillations driven by *Drd3::luc* in C-1300N cells.(mean ±S.E. (n=3)) (B) The period change in C-1300N cells. Each column represents the mean ±S.E. (n=3) (*Bmal1*::Luc vs *DRD3*::Luc；Student‘t Test；N.S) (C) Representative traces of bioluminescent oscillations driven by *Drd3::luc* in C1300N cells with the kuronos (ATTO). The C-1300N cells were transfected with 2 μg of pcDNA (black line) or 2 μg of REV-ERBα (gray line) using Lipofectamin 2000. (pcDNA; $P < 0.05$, cosinor analysis,mean ±S.E. (n=3))

Supplemental Figure 3

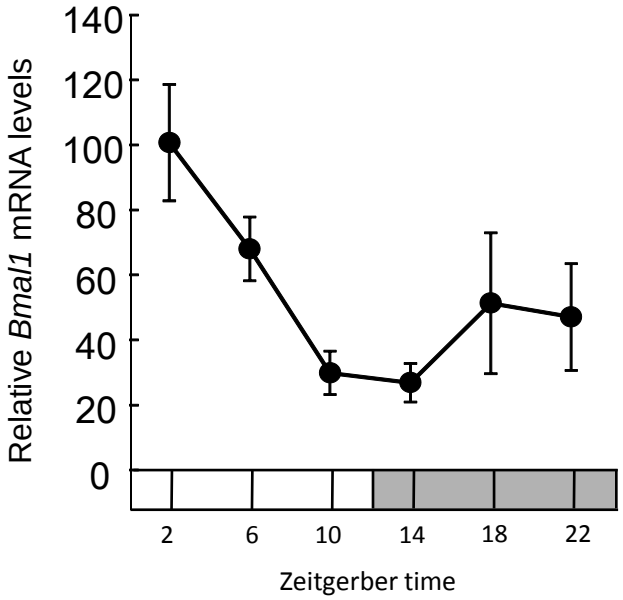

Supplemental Figure 4 Temporal expression profile of *Bmal1* mRNA in the ventral striatum. The data was normalized using β-actin as a control. For intensity plots, the mean value of ZT2 was a set at 100. Each value represents the mean ± S.E. (n=6. $p<0.05$; cosinor analysis)